In situ neutron diffraction measurement of residual stress relaxation in a welded steel pipe during heat treatment

Chen, B. , Skouras , A. , Wang, Y. Q. , Kelleher , J. F. , Zhang, S. Y. , Smith, D. J. , Flewitt, P. E. J. and Pavier, M. J.

Original citation & hyperlink:
Chen, B. , Skouras , A. , Wang, Y. Q. , Kelleher , J. F. , Zhang, S. Y. , Smith, D. J. , Flewitt, P. E. J. and Pavier, M. J. (2014) In situ neutron diffraction measurement of residual stress relaxation in a welded steel pipe during heat treatment. Materials Science and Engineering: A, volume 590 : 374-383
http://dx.doi.org/10.1016/j.msea.2013.10.060

ISSN 0921-5093
DOI 10.1016/j.msea.2013.10.060

In Situ Neutron Diffraction Measurement of Residual Stress Relaxation in a Welded Steel Pipe during Heat Treatment

B. Chen[1,a,*], A. Skouras[a], Y.Q. Wang[a], J.F. Kelleher[b], S.Y. Zhang[b], D.J.Smith[a], P.E.J. Flewitt[c], M.J. Pavier[a]

[a]*Department of Mechanical Engineering, University of Bristol, Bristol BS8 1TR, UK*
[b]*ISIS, Science and Technology Facilities Council, Rutherford Appleton Laboratory, Chilton, Didcot, Oxfordshire, OX11 0QX, UK*
[c]*H.H. Wills Physics Laboratory, University of Bristol, Tyndall Avenue, Bristol, BS8 1TL, UK*

*Corresponding author. Tel.: +44 117 331 5941. Fax: +44 117 929 4423.

E-mail address: bo.chen-2@manchester.ac.uk

Abstract

Many previous studies have presented results on the relaxation of residual stress in a welded component as a result of post weld heat treatment. Techniques such as neutron diffraction and deep hole drilling have been used to measure the residual stress after the heat treatment and compare this with the residual stress for the component in the as-welded condition. The work described in this paper is novel: neutron diffraction is used to measure the relaxation of residual stress continuously as the heat treatment is being carried out. Residual stresses are measured in a butt-welded ferritic steel pipe as the pipe is heat treated to 650°C and then cooled to room temperature. The results identify those parts of the heat treatment that lead to significant stress relaxation and the mechanisms responsible for this relaxation. The techniques developed during this work allow future heat treatments to be optimised to achieve the low levels of residual stress in welded components.

Keywords: Stress relaxation; Post weld heat treatment; Neutron diffraction; In-situ; Steel

1. Introduction

Weldments used in for example nuclear and petrochemical components, when operating at elevated temperatures, have been recognised to be the most susceptible locations to cracking [1-4]. The presence of the welding induced residual stresses and their relaxation as a consequence of high temperature exposure, prior to or during service, were judged to be a

[1] Present address: Materials Performance Centre, The School of Materials, The University of Manchester, Oxford Road, Manchester, M13 9PL

key factor in controlling the susceptibility to cracking [2, 5]. For example, if the relaxation of tensile residual stresses occurs at an inappropriate rate, this can lead to a stress relief cracking during the post weld heat treatment (PWHT) or a reheat cracking during service [3, 4]. A method for the prediction of creep crack initiation in the weldments due to residual stress relaxation can be found in the R5 procedure [6]. One of the inputs required in this prediction is the instantaneous creep strain rate, which is equivalent to the instantaneous relaxation rate of the residual stresses. Thus, it is essential to understand the relaxation rate of residual stresses during PWHT or service at elevated temperatures. The knowledge of the residual stresses after the heat treatment, and thereby the magnitude of the relaxed residual stresses, is insufficient for the structural integrity assessment.

To date, residual stress measurements have been made successfully through the thickness of components or laboratory sized specimens by using mainly four techniques: (i) deep hole drilling [7], (ii) neutron diffraction (ND) [8], (iii) high energy synchrotron X-ray diffraction (HEXRD) [5], and (iv) the contour method [9]. Residual stresses were measured in a 84mm thick welded steel pipe using the deep hole drilling technique, through the wall thickness of the pipe at weld centreline, before and after PWHT [7]. It showed a significant relaxation of the tensile residual stresses after PWHT. Another example is the residual stress measurements undertaken in 25mm a thick compact tension specimen. In this case, the change in residual stress fields was measured before and after the heat treatment, using both the HEXRD and ND techniques [5]. However, both of these studies did not provide a temporal evolution of the residual stresses during the heat treatment.

A few experimental studies have attempted to measure the relaxation of residual stresses during the heat treatment by using diffraction based techniques. Techniques include X-ray diffraction (XRD), HEXRD and ND. Residual stress measurements were undertaken in nanocrystalline aluminium alloy (3mm×3mm×5mm parallelepiped) [10], in nanocomposite metals (1mm^2 in cross-section and 15mm in length) [11], in metal or alloy thin films (typically 50 to 2000nm thick films deposited on substrates) [12, 13], in single phase polycrystalline beryllium (5mm in diameter and 20mm in length) [14], and in laboratory sized specimens manufactured from engineering alloys or metal matrix composites [15-22]. The XRD has a low penetration to the material, ~50μm for aluminium, and the other two have a higher penetration, ~150mm for aluminium [23]. The diffraction angles are usually low for HEXRD (typically 2 to 20°), due to the short wavelength. This results in an

elongated diamond shaped prism for the sampled gauge volume [24]. This limits the strain measurement along three principal vectors at each point to calculate stresses. In contrast, the ND technique uses a cubic sampling gauge volume, determined by the arrangement of the detectors 90° relative to the incident beam [2]. Thus it is possible to characterise the residual stress field at each point of interest.

A critical problem when undertaking a residual stress measurement during the heat treatment is the determination of stress free lattice parameters, which are dependent on the chemical composition, thermo-mechanical history and service history of the materials [2, 25]. XRD residual stress measurement, using a classical $\sin\psi^2$ technique, does not require the knowledge of stress free lattice parameters. However, both the HEXRD and ND techniques require a highly reliable measure of the stress free lattice parameters. When the HEXRD and ND techniques were used for the measurement of residual stresses at elevated temperatures, the use of thermal expansion coefficient (TEC) to predict the stress free lattice parameters was often adopted to avoid of a direct measurement [11, 22]. However, the TEC is a temperature dependent parameter, $\alpha(T)$, and has been normally expressed in the form of either a two-parameter or a three-parameter relationship [26, 27]. In the former, a linear relationship between the TEC and temperature was predicted, whereas the latter gave a non-linear relationship between these two. Although the TECs required in the pressure-volume-temperature (PVT) data have been measured using the in-situ synchrotron X-ray diffraction (HEXRD) [27-29], the materials comprised mainly with a simple constituent, such as ε-iron (ε-Fe), γ-iron (γ-Fe), Fe_3S, FeSi and Fe_3C. This raised a question of whether the predicted temperature dependent stress free lattice parameters could be used for the residual strain/stress derivation in engineering materials.

In the present work, in-situ heat treatment combined with neutron diffraction (ND) residual stress measurement has been performed on two circumferentially butt-welded steel pipes. The temporal change of the welding induced residual stresses together with the temperature dependent stress free lattice parameters have been measured. This was achieved by manufacturing an in-situ stress free sample on the butt-welded pipe. The measured results allow us (i) to understand the instantaneous relaxation of residual stresses during PWHT in the interior of the weld metal and (ii) to validate the prediction of the stress free lattice parameters based on the temperature dependent TEC.

2. Experimental procedure

2.1. General approach

The aim of the work described here is to measure the relaxation of residual stress in a welded steel pipe during heat treatment using neutron diffraction. The heat treatment is applied using electric heating blankets wrapped around the pipe. In this way, the heat treatment can be carried out at the same time as the neutron diffraction measurements.

Our approach taken was guided by the desire to make measurements as rapidly as possible with a small time interval between subsequent measurements. Since the magnitude of residual stresses measured by neutron diffraction relies on the stress free lattice parameters [30], it was also necessary to aim for near simultaneous measurements of the residual stress in the weld and in a stress free sample subjected to the same variation in temperature. The time required for each measurement is controlled by the neutron flux, the thickness of material through which the beam must penetrate and also the desired accuracy of the diffraction peak positions. A customised measurement simulation programme is available at ISIS which allows the design of the procedure to be optimised. By reducing the wall thickness of the pipe to 10mm and by cutting neutron beam access windows in the pipe where possible, the time taken for each measurement could be reduced to 240 seconds, assuming a typical neutron flux.

It was decided to measure the residual stress at only one point during the heat treatment, on the weld centreline and in the mid-thickness of the pipe. Of course, measuring the stress at two points would increase the time interval between subsequent measurements by at least a factor of two. However, a sequence of measurements (five points across the weld centreline) was carried out across the weld before the heat treatment commenced and after it had been completed and the pipe had cooled down.

Each measurement on the stressed weld was followed by a stress free measurement on a corresponding point on the mechanically stress relieved weld where a comb specimen had been cut into the weld to reduce the level of stress to close to zero. Since the position of the beam is fixed, the pipe had to be manipulated between these two measurement positions using a positioning stage. The speed of travel of this positioning stage was limited which

meant that about one minute was required from the end of a measurement on the weld to the start of the stress free measurement on the comb.

It was not feasible to rotate the pipe so that measurements could be made at various orientations. When the principal orientations are identified, strain measurements along these three orientations are sufficient to derive the residual stresses [2]. Thus for the present work, a sequence of measurements was made for one or two orientations on one welded pipe, and then a further sequence of measurements were made for a different orientation on a second pipe.

2.2. Weld specimens

Two nominally identical butt-welded pipes in the as-welded condition were provided by Doosan Power Systems. Each pipe was 300mm long with an outside diameter of 170 mm and a wall thickness of 10mm. The pipes were fully prepared and the multiple-pass welds carried out using combined gas tungsten arc and manual metal arc welding methods. The dimensions of the weld preparation are shown in Figure 1(a). This figure also shows the pattern of weld beads taken from a macrograph of a removed segment of the weld, etched using a 2% Nital solution, Figure 1(b). The root run weld for this butt weldment can be seen in Figure 1(b). The pipes were of C-Mn steel and the weld consumable was Cr-Mo steel. Figures 1(c) and 1(d) show microstructures of the weld and parent material. These microstructures are described in more detail later. The chemical compositions of the parent and weld metal were measured from samples extracted from the pipes and are given in Table 1. No differences were detected between samples extracted from the two pipes. Vickers macro-hardness (Hv10) measurements were undertaken on two weld cross-section samples, detached from pipe 1, before and after the heat treatment.

A comb was cut into each pipe through the centre of the weld to provide a stress free measurement point. The comb was machined using wire EDM with a 0.25mm diameter wire. The geometry of the wire EDM process meant that two combs were machined at the same time, diametrically opposite each other. During the neutron diffraction measurements only one of the combs on each pipe was used. The dimensions of the comb are defined in Figure 2.

To reduce the thickness of material through which the neutron beam would have to penetrate,

various machining operations were carried out on the pipes. Pipe 1 would be used for measurement of hoop strain in the centre of the weld (the *measurement point*) and at the centre of the comb cut into the weld (the *stress free measurement point*) at 90° from the measurement point. Therefore two windows were cut into the wall of the pipe opposite these measurement points. The dimensions of these windows and their locations relative to the measurement points are shown in Figure 3. Pipe 2 would be used for the measurement of axial strain. For the measurement of the strain in the weld the neutron beam does not have to pass through material and therefore no machining needs to be carried out. However, a flat has to be machined around the comb to allow the stress free measurement. The dimension of the flat and its location is shown in Figure 4.

2.3. Neutron diffraction

Neutron diffraction measurements were undertaken using ENGIN-X time-of-flight neutron diffractometer, located at ISIS, Rutherford Appleton Laboratory, UK [30]. A pulsed beam of neutrons with a wide energy range travels to the selected measurement position, and a small fraction of the beam is diffracted into the detectors, located at an angle of $2\theta = 90°$. The wavelength, λ, of the detected neutrons is calculated from their time-of-flight, t, between the moderator and the detector [30]:

$$\lambda = \frac{h}{mL}t \tag{1}$$

where h is the Planck constant, m is the neutron mass and L is the neutron flight path from the moderator to the detector. Thus, the lattice spacing, d, for a specific grain family $\{hkl\}$ in a polycrystalline material can be derived from Bragg's law:

$$d_{hkl} = \frac{h}{2mL\sin\theta}t_{hkl} \tag{2}$$

The presence of the elastic strain changes the magnitude of lattice spacing, d_{hkl}. As a consequence, the evaluation of the elastic strain in each grain family requires a measure of the lattice spacing under the stress free condition, d^0_{hkl}. The strain, ε_{hkl}, is determined from the change in the lattice spacing:

$$\varepsilon_{hkl} = \frac{d_{hkl} - d^0_{hkl}}{d^0_{hkl}} \tag{3}$$

ENGIN-X is a time-of-flight sourced neutron diffractometer allowing multiple diffraction peaks corresponding to the different grain families {*hkl*} can be collected simultaneously. The engineering strain can be then derived from the change in the lattice parameter, a, when a Rietveld refinement is applied to the complete diffraction spectrum [31]. This provides a significant reduction in counting times as well as a good measure of bulk macroscopic strain in an engineering sized component. Residual stresses were derived from the measured three principal strains in the hoop, radial and axial directions for the butt-welded pipe, using Hooke's law. For example, the calculation of the hoop stress is given by:

$$\sigma_h = E\left[\frac{(1-\nu)\varepsilon_h + \nu(\varepsilon_r + \varepsilon_a)}{(1+\nu)(1-2\nu)}\right] \tag{4}$$

where σ_h is the hoop stress, ε_h is the hoop strain, ε_r is the radial strain and ε_a is the axial strain. A value of 205GPa was used for Young's modulus, E, and 0.27 was used for Poisson's ratio.

2.4. In situ heat treatment measurements

The heat treatment was carried out using two electric heating blankets fabricated from ceramic sintered alumina. Each blanket was 500mm wide by 120mm long. These heating blankets were wrapped around the two halves of each pipe with a gap of about 40mm between them, centrally over the weld, to allow access for the neutron beam to the measurement points. Two individual electrical power generators were connected to the heating blankets to supply a continuous heat. Two thermocouples were attached to the pipe within the weld metal region to provide control of the temperature. The whole pipe and heating blankets were wrapped in calcium magnesium silicate insulation with windows cut into the insulation for neutron beam access.

The pipes were each attached to a positioning stage using a water-cooled mounting bracket. Pipe 1 was used for hoop measurements of the lattice parameter at the measurement point and the stress free measurement point. These two measurements of the lattice parameter enable

the variation of the hoop strain to be determined. Pipe 1 was therefore attached to the positioning stage with its axis vertical, as shown in Figure 5. In Figure 5(a) the measurement of the lattice parameter in the centre of the stressed weld is being made using Detector 2. In Figure 5(b) the positioning stage has moved the pipe to the left to measure the stress free lattice parameter using Detector 1.

Pipe 2 was used for axial measurements of the lattice parameter. This pipe was attached to the loading stage with its axis horizontal as shown in Figure 6. Figure 6(a) shows the measurement of the lattice parameter in the axial direction for the stressed weld being made using Detector 2. Simultaneous measurements of the lattice parameter in the radial direction were also possible using Detector 1. In Figure 6(b) the positioning stage has moved the pipe down, to the right and in the direction of the beam to enable the measurement of the stress free lattice parameters. Detector 2 is again used to measure the lattice parameter in the axial direction. Simultaneous measurements are also possible using Detector 1, but for the hoop direction, not the radial direction. Unfortunately, it was not possible to measure the stress free lattice parameter in the radial direction. Therefore, in subsequent calculations the radial strain was obtained based on the lattice parameter measured in the radial direction and the stress free lattice parameter measured in the hoop direction. Table 2 summarises the neutron measurements carried out on both pipes.

The measurements were made using a gauge volume of 4mm×4mm×4mm and a fixed measurement time of 240 seconds. This gave a compromise between frequency of measurement; accuracy, increased by using a longer measurement time; and resolution, increased by a smaller gauge volume. Only one measurement point in the weld metal and the corresponding stress free measurement point were used. The measurement point was in the centre of the weld and in the mid-thickness of the pipe wall, 5mm below the weld surface. Measurements were made at the measurement point and stress free point alternately throughout the heat treatment.

One after the other, the pipes were heated continuously to a temperature of about 650°C, followed by air cooling to room temperature. Figure 7 shows the temperature history experienced by pipe 1. Each temperature point indicates the temperature when a neutron diffraction measurement was made. Also illustrated in Figure 7 are two periods, labelled *dwells* in the figure, where the temperature was held constant: one at 450°C and one at 650°C.

These two periods were used to investigate whether any relaxation in stress occurs over time at constant temperature, for example due to creep. Pipe 2 experienced a similar temperature history to that of pipe 1 except that there was no dwell at 450°C.

Figure 7 also shows evidence of practical problems associated with the experiment. The principal problem encountered was that the electrical supply to the ENGIN-X facility became unstable and was prone to cutting out. This accounts for the reduction in temperature at a time of around 550 minutes into the test in Figure 7. Another problem was that the neutron beam flux varied and could drop to a level where measurements were not able to be made. The gaps in the temperature data in Figure 7, except for the cooling, correspond to such periods when the neutron beam was not operating at normal levels. The plans for the enhancement of the ENGIN-X facility in terms of undertaking this type of novel experiment will be given later.

In addition to the neutron measurements carried out during the heat treatment, measurements were also made at five positions across the weld centreline before and after the heat treatment to provide the distribution of residual stress in the weldment. These measurements were made for the hoop, axial and radial positions and used the same positions on the pipe as for the in-situ measurements.

3. Results

3.1. Microstructure

The weld metal has a nominal composition of 2Cr1Mo steel, Table 1, and comprised individual weld beads containing an approximately equal combination of columnar and equiaxed grain regions. The latter arose from heat treatment as subsequent beads of weld metal were deposited. The microstructure of the equiaxed grain regions is shown in Figure 1(c). The grain size was ~50μm (linear intercept method) and typical of a tempered upper bainite. The heat affected zone extended over a distance of ~3mm from the low alloy steel weld metal into the parent pipe in the direction normal to the fusion line, Figure 1(b). The squares marked in Figure 1(b) indicate positions where the neutron diffraction measurements were undertaken. The square in the centreline indicates the position where at temperature stress relaxation was monitored. The observed microstructure for the parent Carbon-

Manganese steel pipe was ferrite plus pearlite, Figure 1(d).

3.2. Measurement of lattice parameters

The hoop direction measurements of the lattice parameters together with the stress free lattice parameters for pipe 1 are shown in Figure 8. The figure shows the lattice parameters versus the time from the start of the post weld heat treatment, along with the temperature profile. As the temperature increases the difference between the stressed lattice parameters and the stress free lattice parameters reduces, indicating a relaxation of residual stress in the weld metal. The principal mechanism for this relaxation is believed to be the reduction in yield stress with temperature. The Rietveld refinement used to calculate the lattice parameters also provides the fitting error for each data point, but this error was too small to be shown clearly on the figure.

For the dwell period at 450°C there was no real change in the lattice parameters for the measurement and stress free positions, Figure 8. However, for the dwell period at 650°C the lattice parameter at the measurement position reduced to a smaller value while the parameter at the stress free position remained the same, see the second dwell period in Figure 8. These results suggest that some stress relaxation occurs at 650°C, presumable due to a creep mechanism, while no such relaxation occurs at the lower temperature of 450°C. Once the pipe has been cooled to room temperature, the two measurements of lattice parameters are close to each other, indicating that a majority of the residual stress has been relaxed.

During heat treatment, the neutron diffraction measurements for the stressed and stress free positions were made alternately. During the heating phases of the experiment therefore these two measurements were made at different temperatures. Three sets of stress free lattice parameters were measured during these tests: one for pipe 1 in the hoop direction and two for pipe 2 in the hoop and axial directions (Figure 9). Least squares fits through each set of measured data were used to obtain the corresponding temperature dependent stress free lattice parameters. This allowed a direct comparison of the lattice parameters in terms of stressed and stress free conditions at the same temperature when the residual strain was evaluated. Figure 9 shows the least squares fit for pipe 1.

The least squares fitting parameters for each set of data are shown in Table 3. These

parameters are defined by

$$a_0 = b_1 T + b_2 T^2 + c \tag{5}$$

where a_0 is the stress-free lattice parameter and T is the temperature in °C. A comparatively small value for the parameter b_2 has been obtained indicating a weak dependence of the thermal expansion coefficient with temperature. All three sets of data show a similar gradient but are offset from each other, as shown by the c value in Table 3. This is believed to be a result of a slightly different composition of the weld metal from point to point. The chemical composition of the weld in Table 1 only represents an average value across the weld.

3.3. Measurement of residual stress

The measurements for the hoop direction lattice parameter at the stressed position of pipe 1 were combined with the stress free lattice parameter calculated by Eq. (5) to evaluate the development of the hoop strain during the heat treatment. The least square fitting obtained parameters are given in Table 3. The result is shown in Figure 10. Representative error bars are shown for the initial measurement and the measurement at the end of the heat treatment. The size of the error bars were determined from the size of the variation in the stress-free lattice parameters in Figure 9 and are of the order ±150 μ□. The size of this error is much larger than the fitting error calculated by the Rietveld refinement. The hoop strain generally reduces during the heat treatment. Some further changes in hoop strain occur during cooling as a consequence of a difference between the thermal expansion coefficients of the parent and weld metal.

The calculations for the hoop strain during the heat treatment were repeated for the axial and radial directions, although these axial and radial strain results are not presented here. The calculations for the axial direction used the measurements on pipe 2. For the radial direction, again the measurements for pipe 2 were used except that no stress free measurement was made for the radial direction thus the axial stress free measurement was used instead. These three measurements of strain were combined to provide the change in residual stress using Eq. (4). Figure 11 shows the resulting residual stresses during heat treatment. In this figure, the variation of residual stress versus temperature is shown rather than versus elapsed time. This is because the variation of temperature with time that was achieved during the tests was not

exactly the same for the two pipes. The data for 650°C are the stresses at the end of the dwell. Figure 11 shows that initially the hoop stress has the highest value, followed by the axial and then the radial stress. After heat treatment and after cooling to room temperature, the residual stresses along all three directions relax to similar values, as indicated on the Figure 11. The error bars shown in Figure 11 are calculated from the errors in the strain measurements, reflecting the spread of the stress free measurements of Figure 9.

In addition to the measurements during heat treatment, a series of measurements across the weld metal centreline were undertaken to provide a distribution of the residual stresses in the weldment before and after heat treatment. As shown by the sequences in Figure 1(b), five measurements were made 5mm apart across the weld, starting from a point 10mm from the weld centreline. The measurements 10mm from the weld centreline are within the parent metal while those 5mm from the centreline are close to the fusion boundary. Figure 12 shows the residual stress before heat treatment and Figure 13 after heat treatment. Again, before heat treatment the magnitude of the hoop stresses is generally higher than the axial and radial stresses. After heat treatment the residual stresses have relaxed to much lower values. The results show an asymmetry resulting from the order in which the weld beads were laid down which has been observed in other work [32]. The weld centreline measurements in Figure 13 for the after heat treatment condition are the same as those shown in Figure 11.

3.4. Hardness measurements

Figure 14 shows the results of the Hv10 macro-hardness measurement across the weld cross-section before and after heat treatment. The measurements span the same distance across the weld as the residual stress measurements, which have been schematically shown in Figure 1(b). The weld metal has a higher hardness than the parent, Figure 14. The higher hardness in the weld metal is attributed to the bainitic microstructure, Figure 1(c). The change in hardness is consistent with the presence of weld metal, heat affected zone and parent metal, Figure 1(b). After heat treatment both weld and parent hardness reduce to lower values. The higher hardness observed in the weld metal is consistent with the tempered bainitic microstructure in this region. The asymmetry in the residual stresses is not evident in the hardness results. Since hardness is a function of the yield or flow stress of the material these measurements provide a comparison of the relative properties across the weldment. These data are important since the relative strengths of the weld metal, heat affected zone and parent

control the residual stresses developed in the weld metal, particularly during cooling.

4. Discussion

We emphasise that the in-situ measurements were undertaken only in the weld metal region, Figure 1(b). The measurements were made alternately between the stressed and stress free positions in the weld. The results show that a significant proportion of the residual stress is relaxed instantaneously by an increase in temperature, Figures 10 and 11. The mechanism for this change has been identified as a reduction in the yield stress of the material with temperature. As the temperature is increased, the residual stresses relax until they are on the yield surface corresponding to the current temperature. Evidence for this mechanism can be seen in Figure 15. This figure shows the von Mises equivalent stress calculated from the measured hoop, axial and radial residual stresses during heat treatment. This von Mises equivalent stress is compared with the results of existing work where the 0.2% proof stress of uniaxial specimens cut from annealed steel tubing and steel plate was measured at different temperatures, Figure 15. The material used for these uniaxial tests was a 2.25% CrMo steel which is not exactly equivalent but close to the weld metal of this work, Table 1 [33]. Depending on the heat treatment a range of yield stresses were obtained. The results in the Figure 15 show the maximum and minimum values. Furthermore, the residual stresses in the weld will be affected by the behaviour of the parent material which has a different composition to that of the weld metal.

The derivation of residual stress from strain requires measurements of strain in three principal strain directions, presuming the principal directions are known in advance. This indicates that the measurement of one specimen alone is insufficient to provide the residual stress, unless a positioning stage is available that allows the specimen to be rotated in space. For the case of the ENGIN-X facility at ISIS where two neutron detectors are installed, measurement on two nominally identical specimens are necessary. In practice it is not possible to maintain the same heating rate for each specimen. Furthermore, measurements of residual stress in welded components vary from location to location, even for a single component [34]. Therefore it is not possible to measure the residual stress relaxation as a function of time with great accuracy.

Post weld heat treatment is a widely used industrial procedure to relieve the welding induced

residual stresses in weldments [3, 4] and has been found to decrease the susceptibility of the welded components to failure during service. The selection of the heat treatment parameters, such as maximum temperature, heating rate, cooling rate and dwell time at maximum temperature have been based on experience. This has limited the transferability of the knowledge from one specific weldment to another. For example many austenitic stainless steel welded components have not been subjected to a post weld heat treatment because the resources have not been available to carry out the expensive programme of testing to find the best heat treatment parameters [35]. In addition, failures of austenitic stainless steel welded components do occur, either during service or sometimes during the heat treatment itself [3, 4, 36, 37]. Neutron diffraction techniques allow a high penetration into thick section welded steel components and offer a unique opportunity to measure the stress state in the interior of a weldment during heat treatment. The rate of residual stress relaxation can be measured and therefore the susceptibility of the weldment to stress relief or reheat cracking can be assessed.

The main limitation of the current experiment is that the measurement time for each point takes 240 seconds, so only one point on the weld metal and one point on the stress free sample were measured during the heat treatment. There are a couple of ways to improve this type of experiment. First, the change of stress free lattice parameter has been shown to be in a linear relationship with the temperature in this case, as indicated in Table 3 and Figure 9. The number of stress free lattice parameter measurements thus can be reduced, as long as the data are sufficient to provide a linear prediction between temperature and stress free lattice parameter. This leads to a fact that more measurement points can be selected across the weld centreline on the pipe. Second, event mode data requisition will be available on the beamline in the near future, which allows the user to record a long period of measurement time, and then slice the data with different time intervals. This gives the flexibility of what counting time to choose for the measurement. The advantage of using an event mode for the stress relaxation due to creep has been reported recently by Wang et al [38]. Finally, the neutron diffraction measurement can be run with higher frequency, which will double the flux being used, but the time-of-flight range will be narrowed (e.g. only a couple of peaks can be measured).

5. Conclusions

The present study has shown that it is possible to make measurements of the evolution of

residual stress during heat treatment of a realistic welded engineering component. Previous work has only compared residual stress before heat treatment with the residual stress after heat treatment. Our results show that the residual stress relaxes as the temperature increases due to the reduction in the yield stress with temperature. The results also show for higher temperatures, a relaxation occurs with time at constant temperature. This is associated with creep at high temperature. In principle, measurements such as those reported here provide a methodology for optimising the heat treatment of welded components.

Acknowledgements

Attempting an in-situ neutron diffraction measurement of stress relaxation during heat treatment was initially suggested by Dr Anna Paradowska, formerly at ISIS but now at ANSTO. Dr Bo Chen is grateful for financial support from EDF Energy plc. We are grateful to Dr Peter Barnard of Doosan Power Systems for the provision of the welded pipes. We acknowledge the assistance of Dr Saurabh Kabra, ISIS, and Mr Carlos Garza, University of Bristol, with the neutron diffraction measurements.

References

[1] P.J. Withers, Rep. Prog. Phys., 70 (2007).
[2] B. Chen, P.E.J. Flewitt, D.J. Smith, Mater. Sci. Eng. A, 527 (2010) 7387-7399.
[3] A. Dhooge, A. Vinckier, Weld. World, 30 (1992) 44-71.
[4] A. Dhooge, Weld. World, 41 (1998) 206-219.
[5] M. Turski, P.J. Bouchard, A. Steuwer, P.J. Withers, Acta Mater, 56 (2008) 3598-3612.
[6] R.A. Ainsworth, Int. Mater. Rev., 51 (2006) 107-126.
[7] D.J. Smith, P.J. Bouchard, D. George, J. Strain Anal., 35 (2000) 287-305.
[8] A.J. Allen, M.T. Hutchings, C.G. Windsor, C. Andreani, Adv. Phys., 34 (1985) 445-473.
[9] D.W. Brown, T.M. Holden, B. Clausen, M.B. Prime, T.A. Sisneros, H. Swenson, J. Vaja, Acta Mater, 59 (2011) 864-873.
[10] I. Lonardelli, M. Zadra, G. Ischia, J. Gomez Barreiro, M. Bortolotti, A. Molinari, J. Alloys Compd., 486 (2009) 653-659.
[11] J.B. Dubois, L. Thilly, P.O. Renault, F. Lecouturier, M. Di Michiel, Acta Mater, 58 (2010) 6504-6512.
[12] E. Eiper, J. Keckes, K.J. Martinschitz, I. Zizak, M. Cabie, G. Dehm, Acta Mater, 2007 (2007) 1941-1956.
[13] H. Kostenbauer, G.A. Fontalvo, M. Kapp, J. Keckes, C. Mitterer, Surf. Coat. Technol., 201 (2007) 4777-4780.
[14] D.W. Brown, T.A. Sisneros, B. Clausen, S. Abeln, M.A.M. Bourke, B.G. Smith, M.L. Steinzig, C.N. Tome, S.C. Vogel, Acta Mater, 57 (2009) 972-979.
[15] A. Madgwick, T. Mori, P.J. Withers, Mater. Sci. Eng. A, 333 (2002) 232-238.
[16] P. Jencus, J. Polak, P. Lukas, O. Muransky, Physica B: Condensed Matter, 385 (2006) 597-599.
[17] H. Choo, P. Rangaswamy, M.A.M. Bourke, Scripta Mater., 42 (2000) 175-181.
[18] G. Bruno, M. Ceretti, E. Girardin, A. Giuliani, A. Manescu, Scripta Mater., 51 (2004) 999-1004.
[19] A. Evans, S.B. Kim, J. Shackleton, G. Bruno, M. Preuss, P.J. Withers, Int. J. Fatigue, 27 (2005) 1530-1534.
[20] P. Juijerm, I. Altenberger, Scripta Mater., 55 (2006) 1111-1114.
[21] H. Lee, S. Mall, Mater. Sci. Eng. A, 366 (2004) 412-420.
[22] R.J. Klassen, K.T. Conlon, J.T. Wood, Scripta Mater., 48 (2003) 385-389.
[23] P.J. Withers, H.K.D.H. Bhadeshia, Mater. Sci. Tech., 17 (2001) 355-365.
[24] P.J. Withers, M. Turski, L. Edwards, P.J. Bouchard, D.J. Buttle, Int. J. Press. Vessels Piping, 85 (2008) 118-127.
[25] A.D. Krawitz, R.A. Winholtz, Mater. Sci. Eng. A, 185 (1994) 123-130.
[26] Properties and Selection: Iron, Steels, and High-Performance Alloys, Vol. 1 of ASM Handbook, ASM International, 10 ed., 1993.
[27] B. Chen, L.L. Gao, K.I. Funakoshi, J. Li, Proc. Natl. Acad. Sci. U.S.A., 104 (2007) 9162-9167.
[28] T. Uchida, Y.B. Wang, M.L. Rivers, S.R. Sutton, J. Geohys. Res., 106 (2001) 21799-21810.
[29] L.S. Dubrovinsky, S.K. Saxena, P. Lazor, Phys. Chem. Minerals, 25 (1998) 434-441.
[30] J.R. Santisteban, M.R. Daymond, J.A. James, L. Edwards, J. Appl. Cryst., 39 (2006) 812-825.
[31] M.R. Daymond, M.A.M. Bourke, R.B. Von Dreele, B. Clausen, T. Lorentzen, J. Appl. Phys., 82 (1997) 1554-1562.
[32] G. Hilson, S. Simandjuntak, P.E.J. Flewitt, K.R. Hallam, M.J. Pavier, D.J. Smith, Int. J. Press. Vessels Piping, 86 (2009) 748-756.
[33] Mechanical Properties Test Data for Structural Materials Quarterly Progress Report for Period Ending October 31, 1976, ORNL-5237, Oak Ridge National Laboratory.
[34] A. Skouras, M.J. Peel, A.M. Paradowska, P.E.J. Flewitt, M.J. Pavier, Int. J. Press. Vessels Piping, 101 (2013) 143-153.
[35] F. Vakili-Tahami, D.R. Hayhurst, Phil. Mag. A, 87 (2007) 4383-4419.
[36] R.D. Thomas JR, Weld. J., Suppl. (1984) 355-368.
[37] R.D. Thomas JR, Weld. J., 63 (1984) 24-32.
[38] H. Wang, B. Clausen, C.N. Tome, P.D. Wu, Acta Mater, 61 (2013) 1179-1188.

Tables

Table 1 Chemical compositions of the weld metal and parent metal (wt.%)

Material	C	Si	Mn	P	S	Cr	Mo	V	Ni	Al	Cu	Ti
Weld	0.10	0.32	0.80	0.011	0.004	1.98	0.82	0.01	0.03	0.01	0.03	0.01
Parent	0.25	0.27	0.54	0.017	0.007	0.04	0.01	0.01	0.02	0.02	0.01	0.01

Table 2 Summary of neutron diffraction measurement directions carried out for the two pipes

Sample	Lattice parameter, a			Stress free lattice parameter, a_0		
	hoop	*axial*	*radial*	*hoop*	*axial*	*radial*
Pipe 1	✓	×	×	✓	×	×
Pipe 2	×	✓	✓	✓	✓	×

Table 3 Parameters in the least squares fit for the stress-free lattice parameter, a_0, obtained from each individual pipe

Sample Name	b_1 (10^{-15} m/°C)	b_2 (10^{-19} m/°C^2)	c (10^{-10} m)
Pipe 1 (hoop)	4.4±0.1	-4.8±1.8	2.8677±0.0001
Pipe 2 (axial)	4.1±0.2	-0.6±0.0003	2.8673±0.0001
Pipe 2 (hoop)	4.1±0.2	-3.8±3.9	2.8667±0.0001

Figure Captions

Figure 1 (a) Dimensions of the weld preparation and approximate position of the weld beads (Details of weld.jpg); (b) macrograph of the weld cross-section showing the neutron diffraction measurement positions (squares) across the weld centreline; (c) low alloy steel weld metal microstructure showing a typical bainitic phase; (d) parent metal microstructure showing a typical mixture of ferrite and pearlite phases. (macrograph of the weld cross-section together with microstutures.jpg)

Figure 2 Dimensions of the comb specimen (Details of comb.jpg)

Figure 3 Dimensions of pipe 1 and the two neutron access windows machined into the pipe (Dimensions of pipe 1.jpg)

Figure 4 Dimensions of pipe 2 showing the flat machined into the pipe (Dimensions of pipe 2.jpg)

Figure 5 The arrangement of pipe 1 relative to the neutron beam for measurements of hoop strain (a) stress measurement and (b) stress free measurement (Neutron beam path for pipe 1.jpg)

Figure 6 The arrangement of pipe 2 relative to the neutron beam for measurements of axial and radial strain (a) stress measurement and (b) stress free measurement (Neutron beam path for pipe 2.jpg)

Figure 7 Measured temperature during the post weld heat treatment for pipe 1 (Temperature during PWHT.jpg)

Figure 8 Hoop direction lattice parameters for the measurement and stress free positions from pipe 1 (Lattice parameters during PWHT.jpg)

Figure 9 Stress free measurements of lattice parameter versus temperature from pipes 1 and 2 (Stress free lattice parameter.jpg)

Figure 10 The measured hoop strain during heat treatment for pipe 1 (Hoop strain during PWHT.jpg)

Figure 11 Measured residual stress during heat treatment (Residual stress

during PWHT.jpg)

Figure 12 Residual stress variation across the weld before heat treatment (As welded residual stress.jpg)

Figure 13 Residual stress variation across the weld after heat treatment (Residual stress after PWHT.jpg)

Figure 14 Distribution of the Vickers macro-hardness (Hv10) across the weld, before and after heat treatment (Hardness measurments.jpg).

Figure 15 Comparison of the variation of the von Mises equivalent stress measured during the heat treatment with the variation of yield stress with temperature measured in uniaxial specimens (Yield stress versus temperature.jpg)

Figure1(a)
Click here to download high resolution image

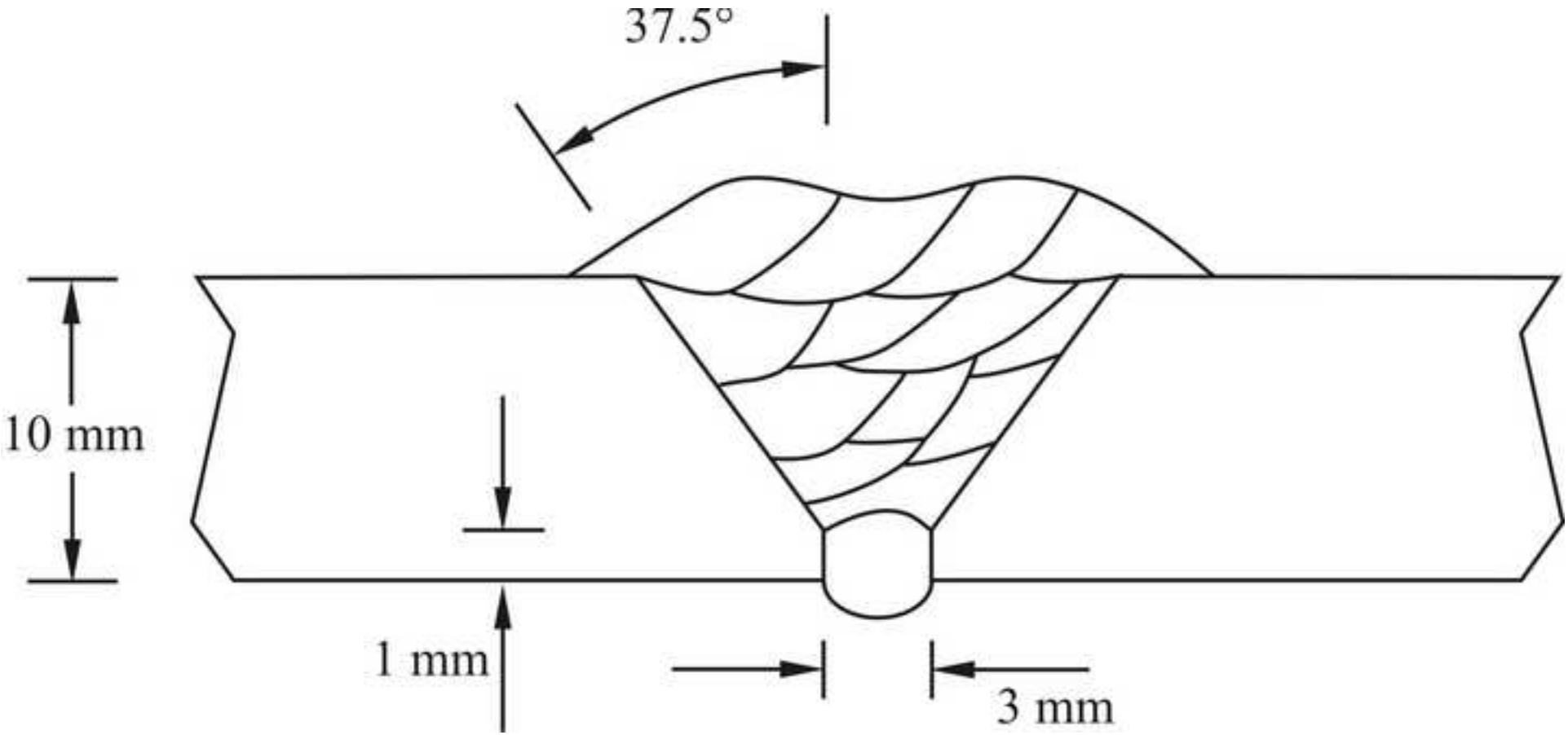

Figure 1 (b) to (d)
Click here to download high resolution image

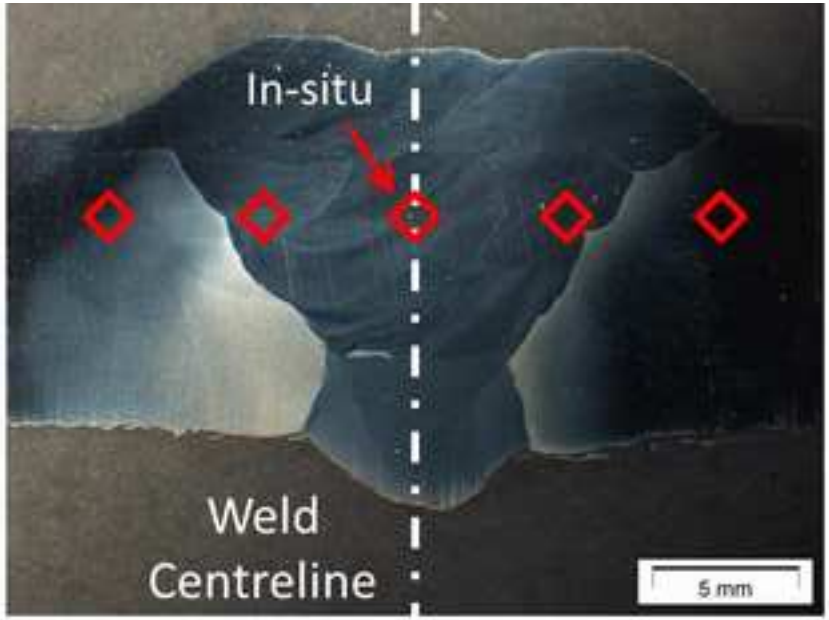

(b)

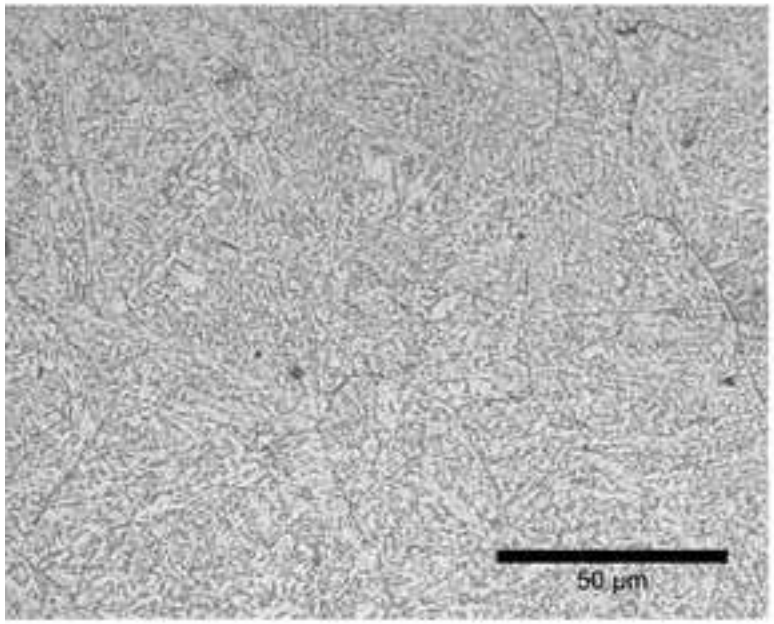

(c)

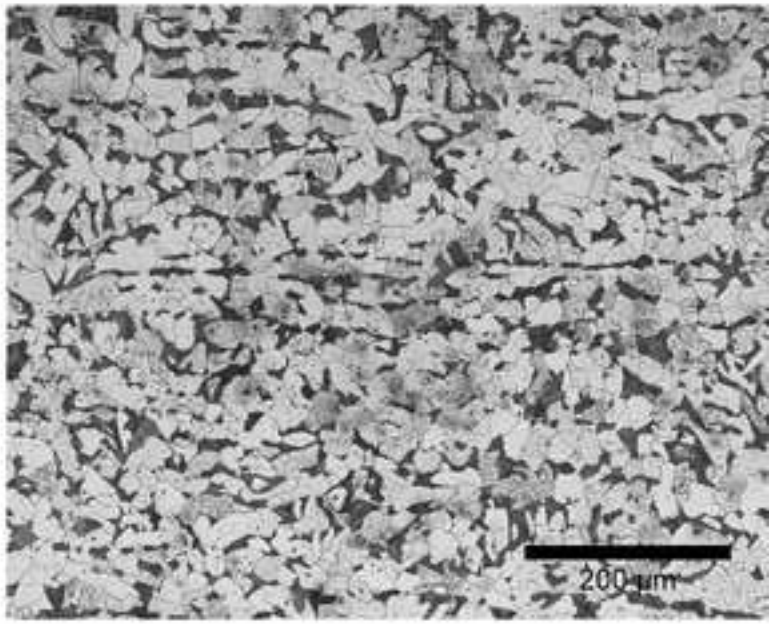

(d)

Figure 2

Click here to download high resolution image

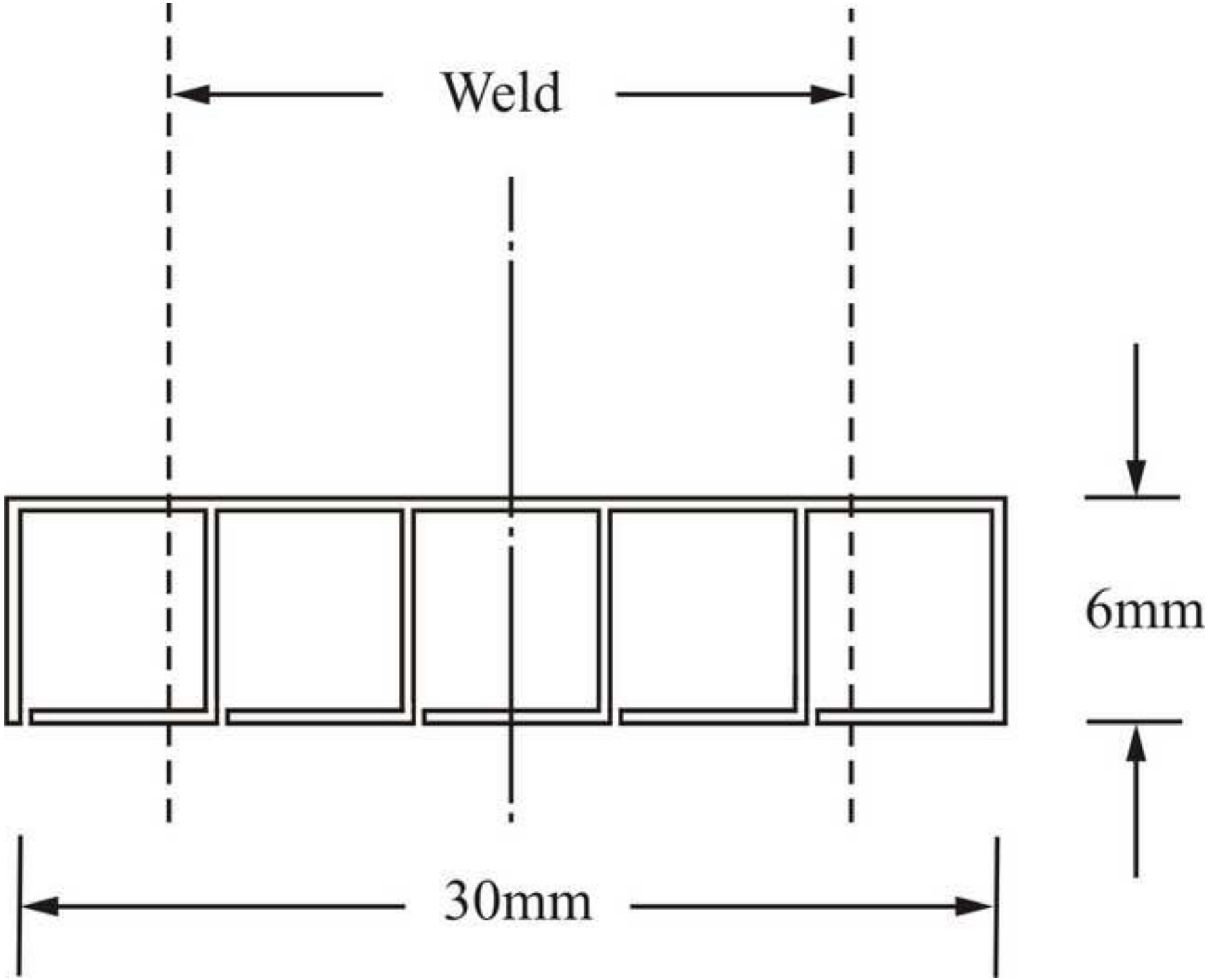

Figure 3
Click here to download high resolution image

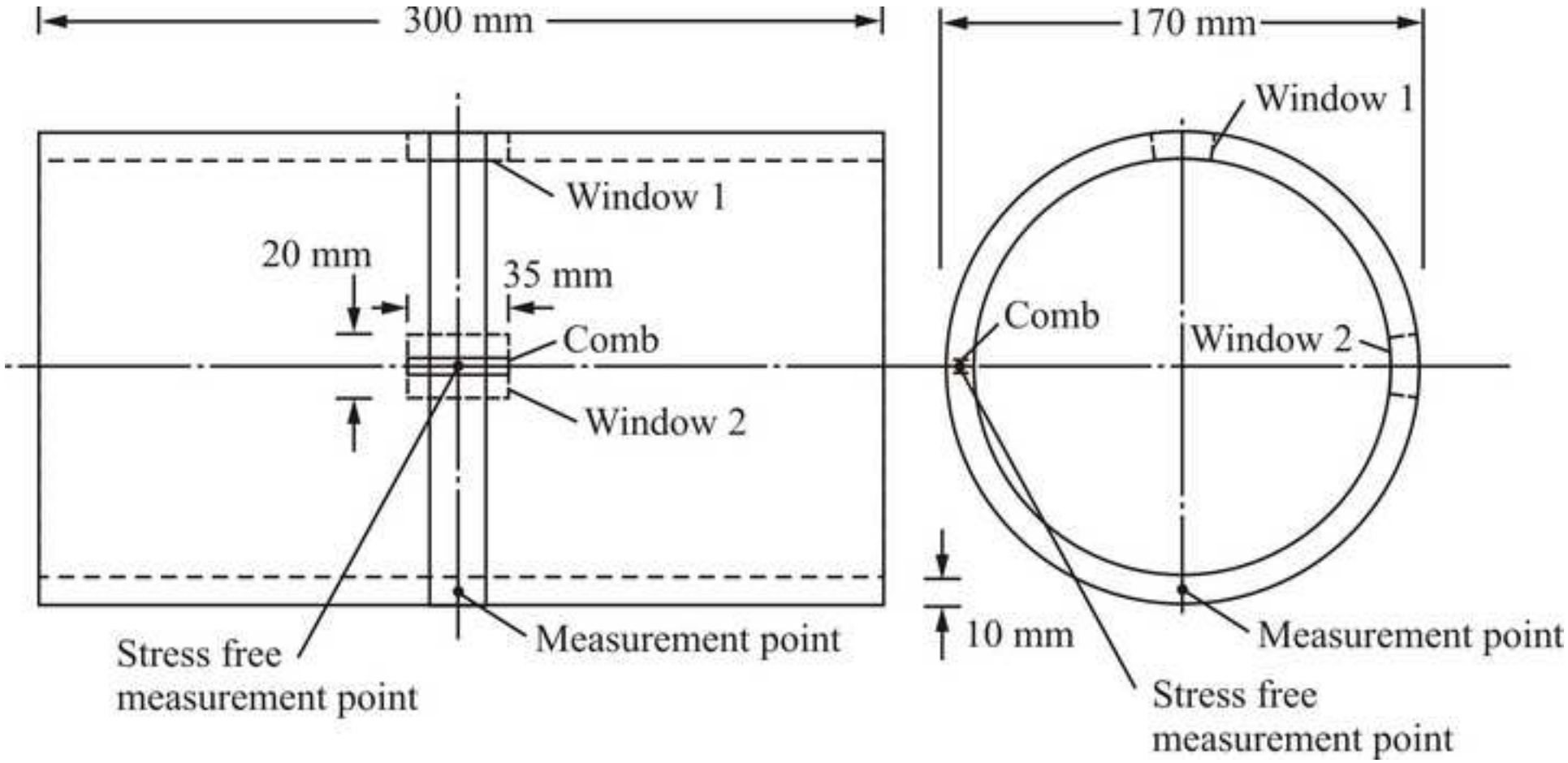

Figure 4
Click here to download high resolution image

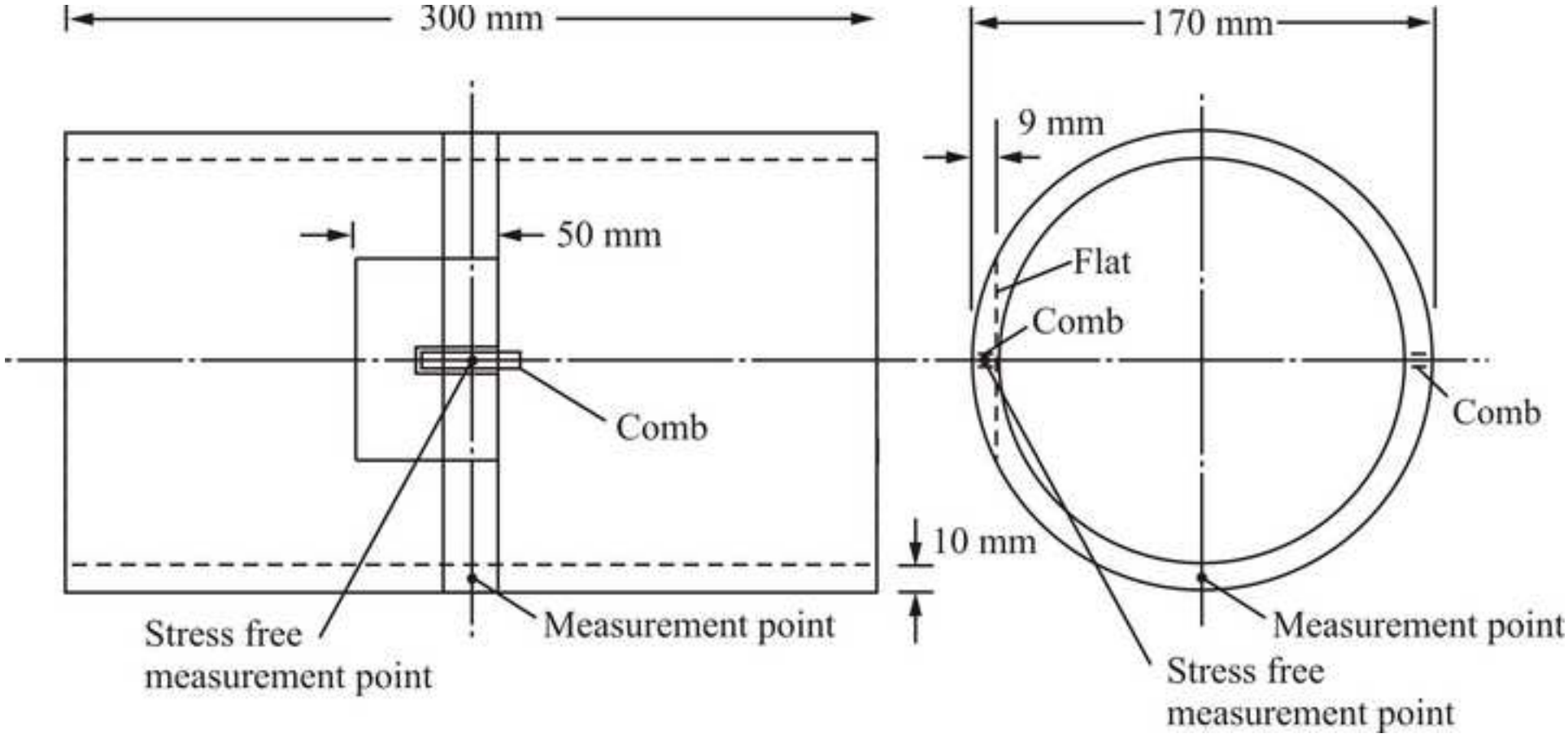

Figure 5
Click here to download high resolution image

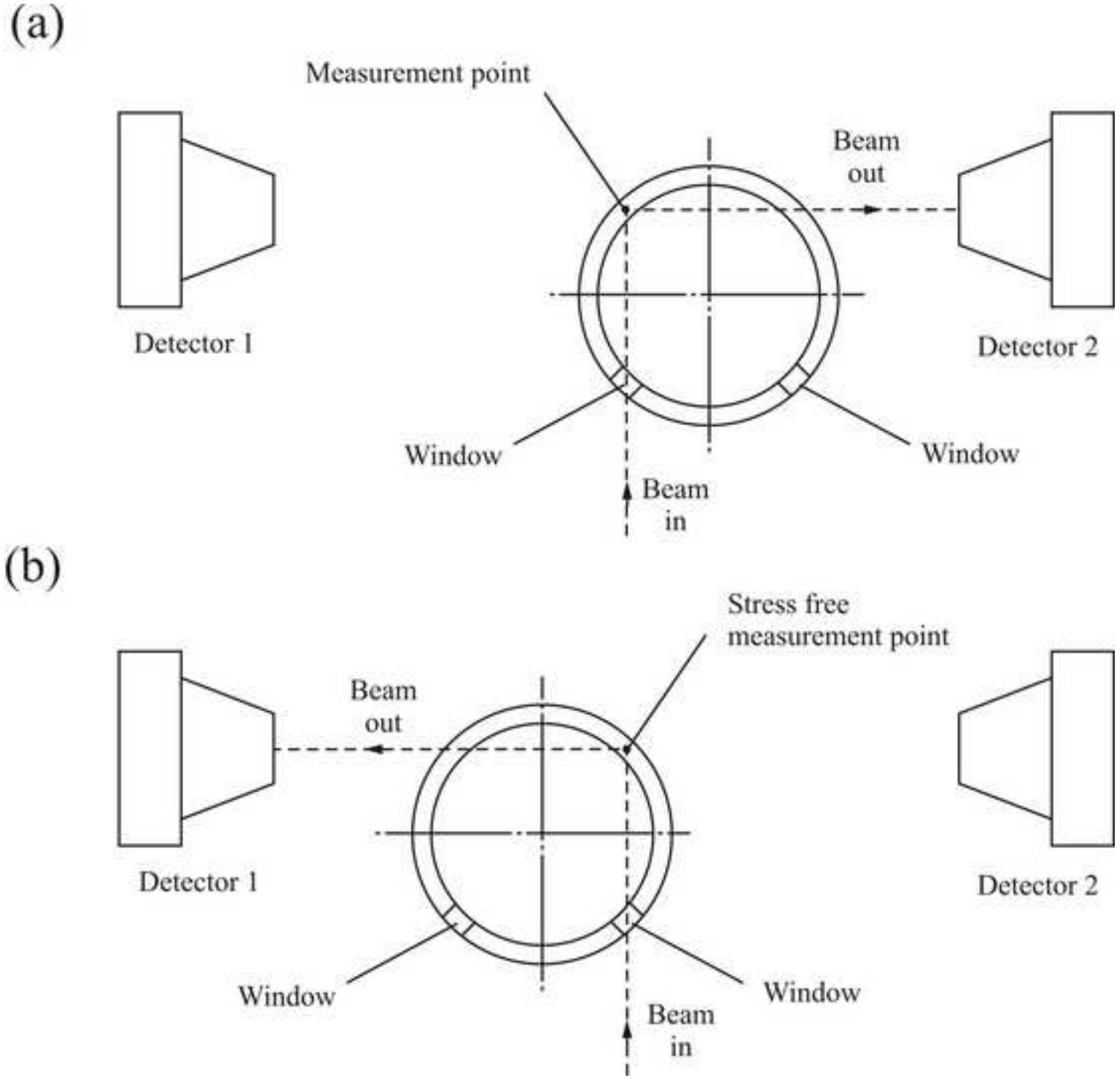

Figure 6
Click here to download high resolution image

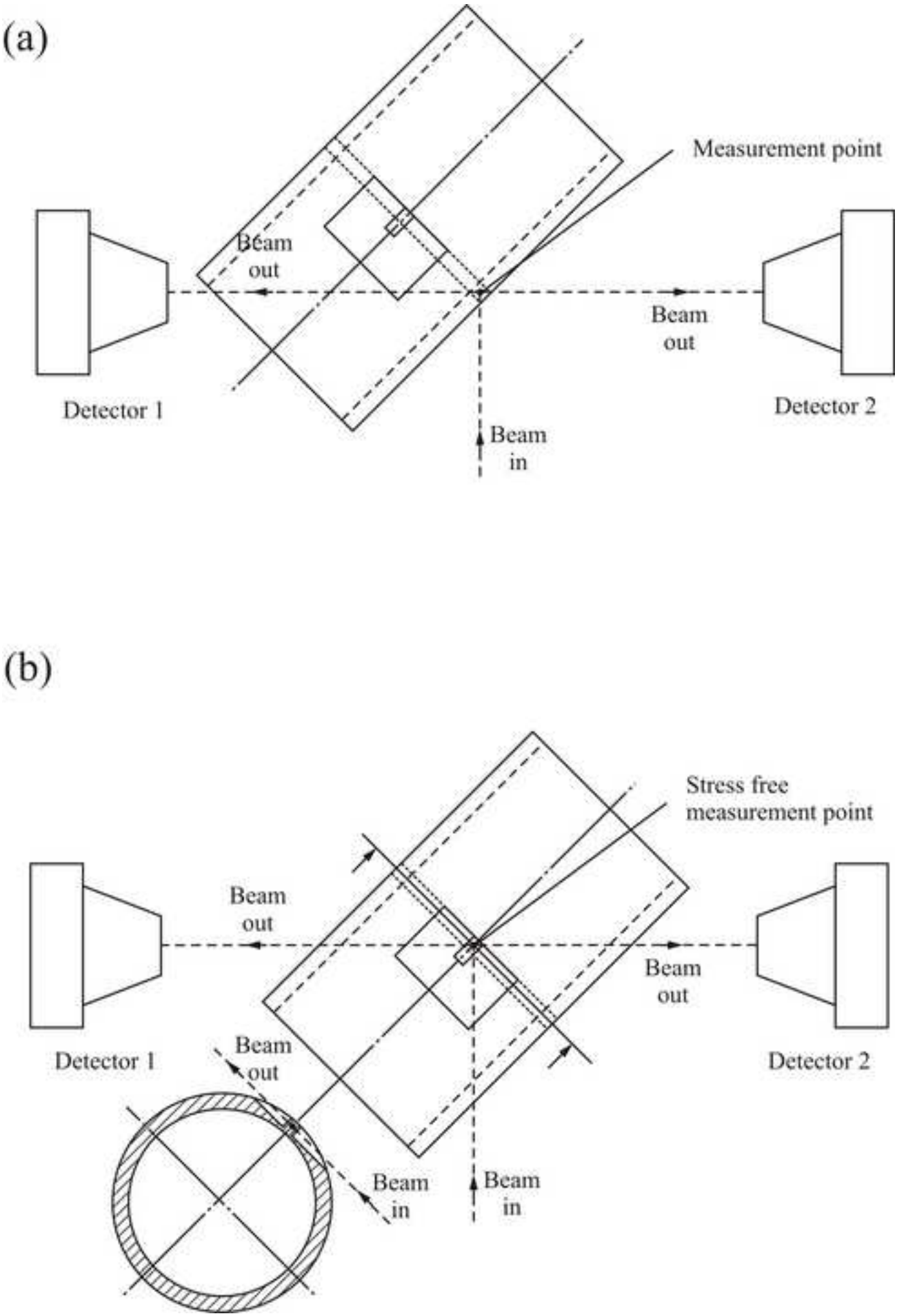

Figure 7

Click here to download high resolution image

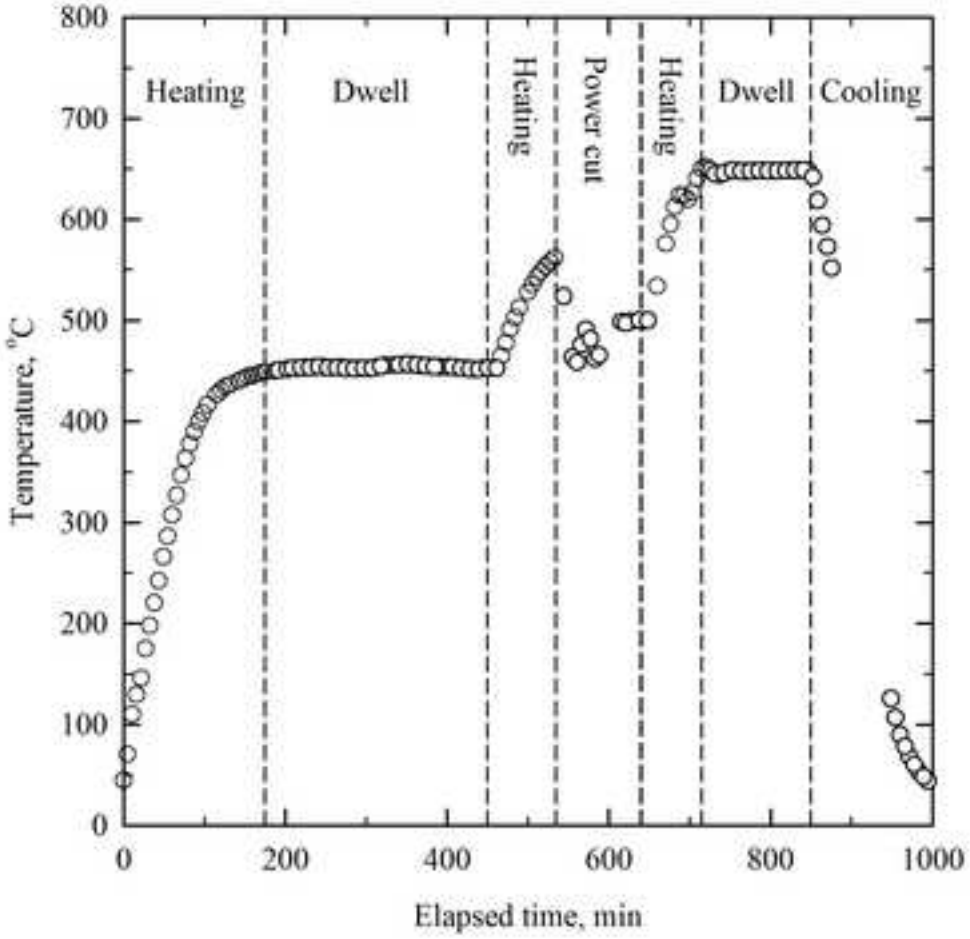

Figure 8

Click here to download high resolution image

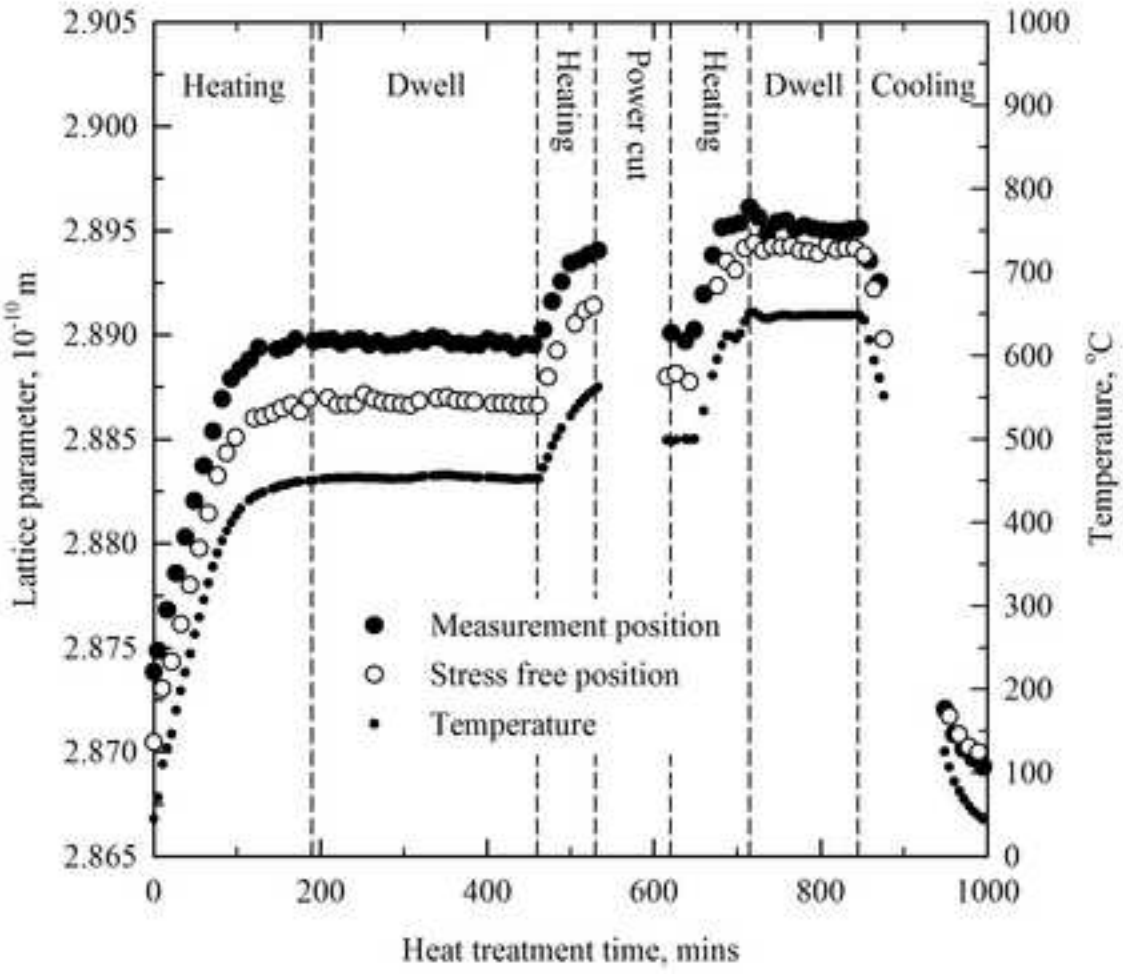

Figure 9

Click here to download high resolution image

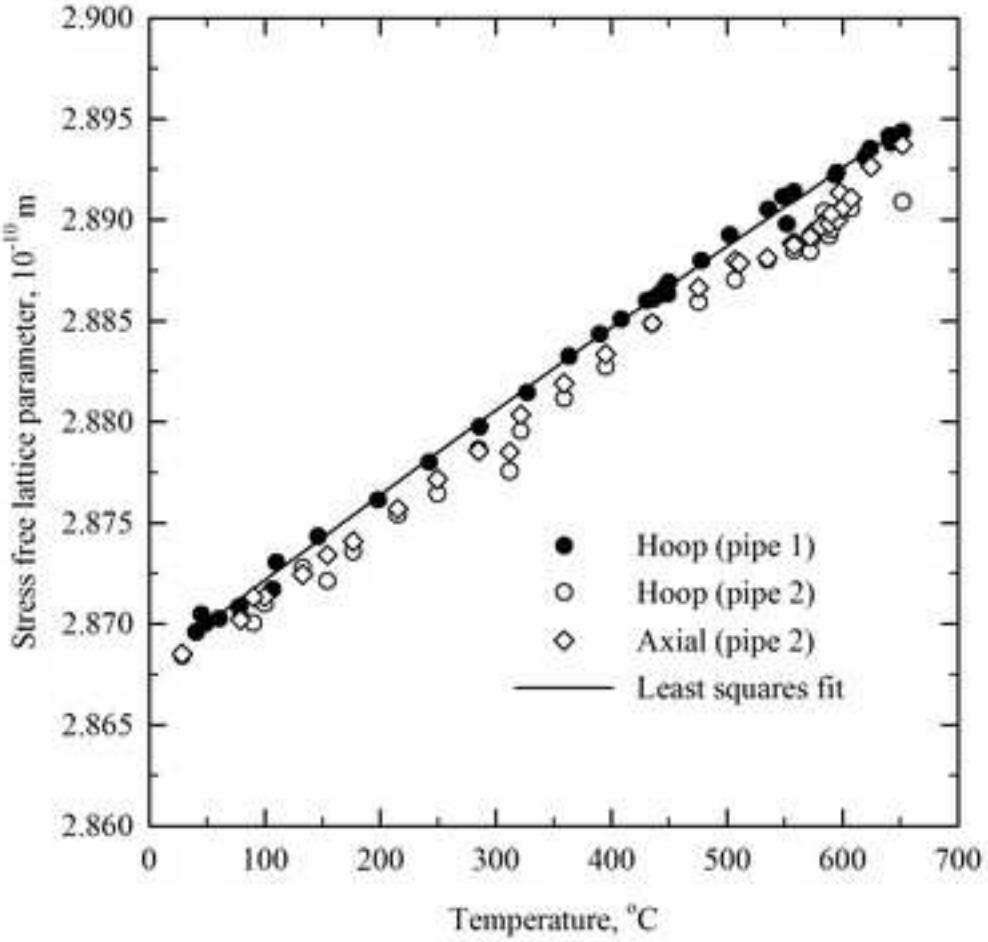

Figure 10

Click here to download high resolution image

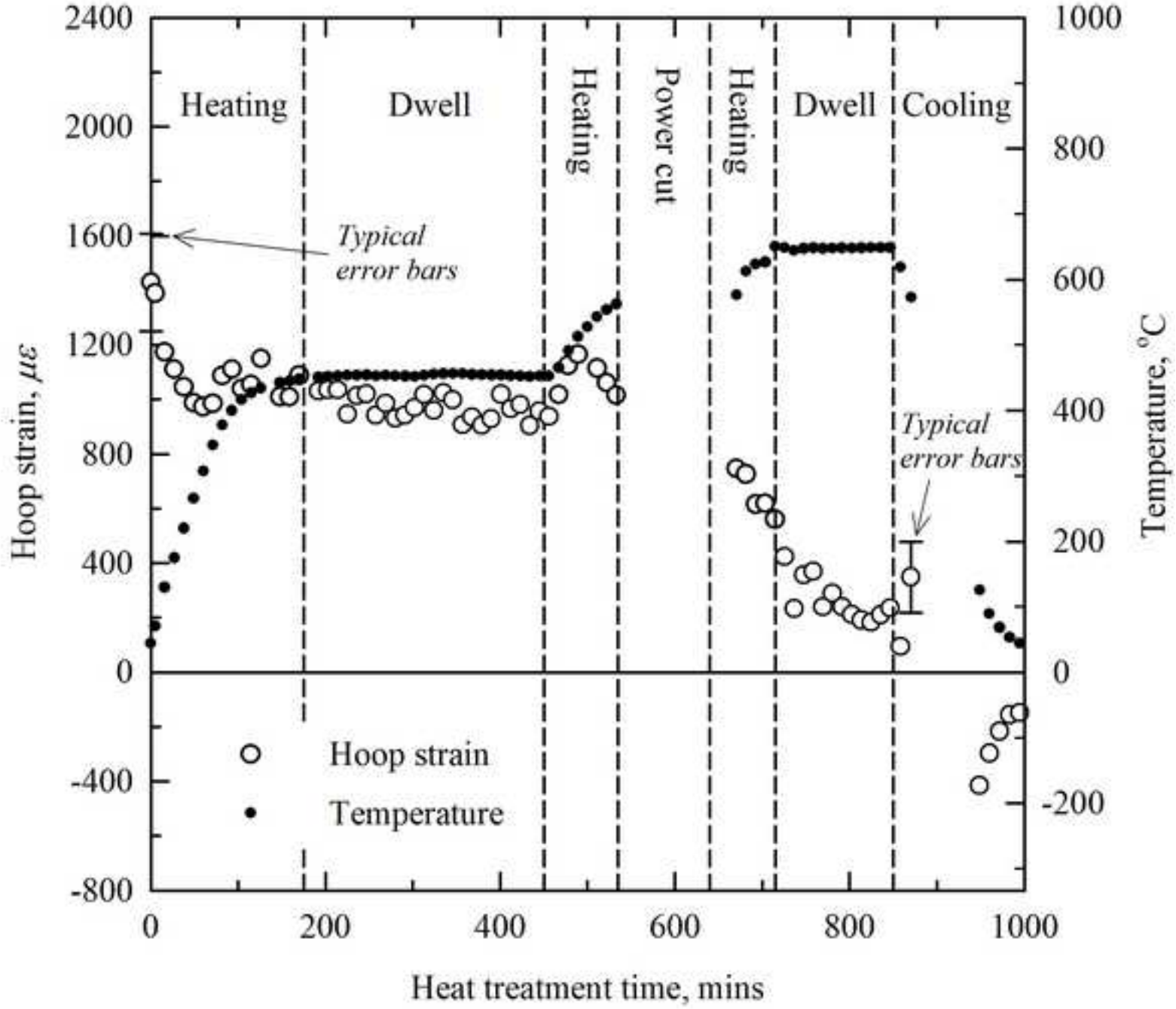

Figure 11
Click here to download high resolution image

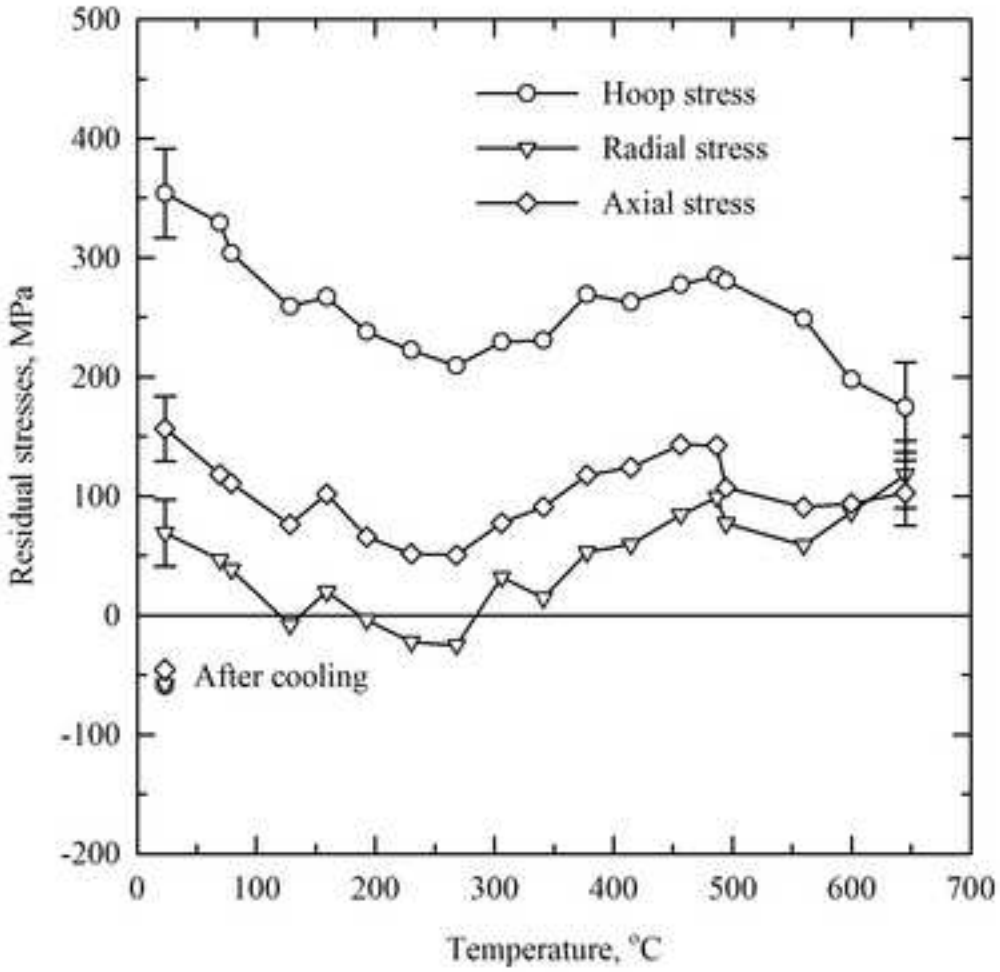

Figure 12
Click here to download high resolution image

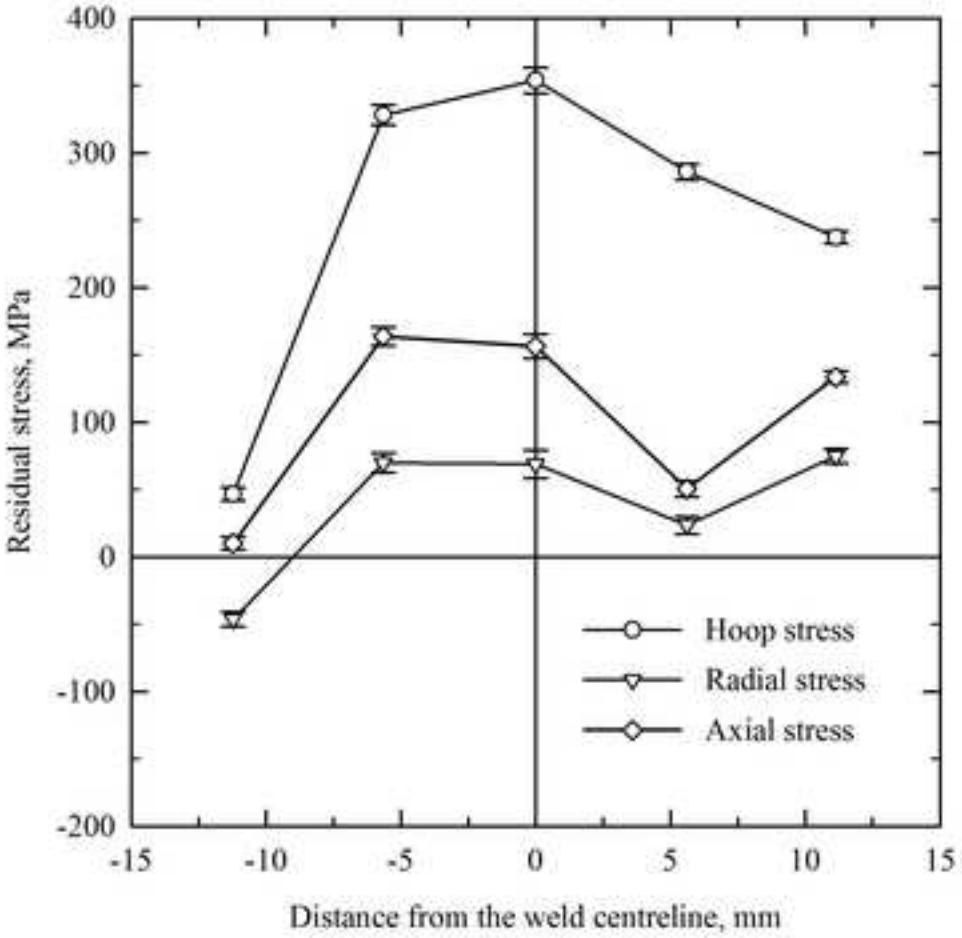

Figure 13
Click here to download high resolution image

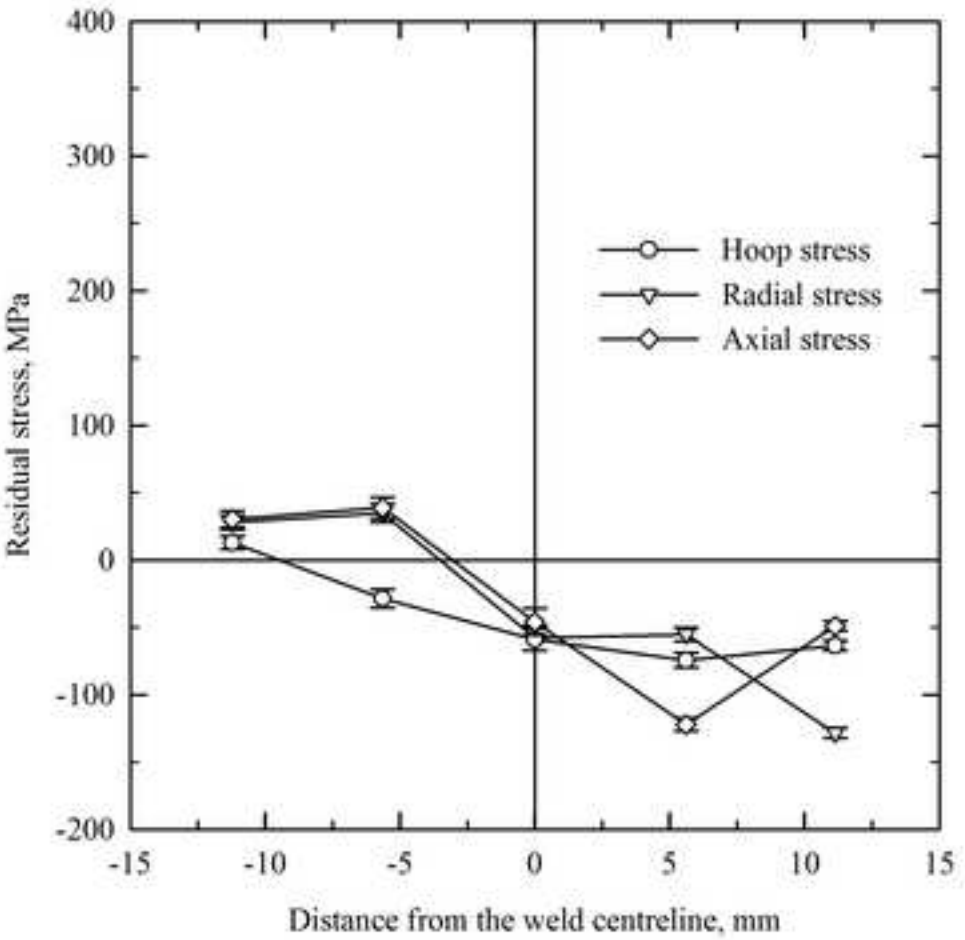

Figure 14
Click here to download high resolution image

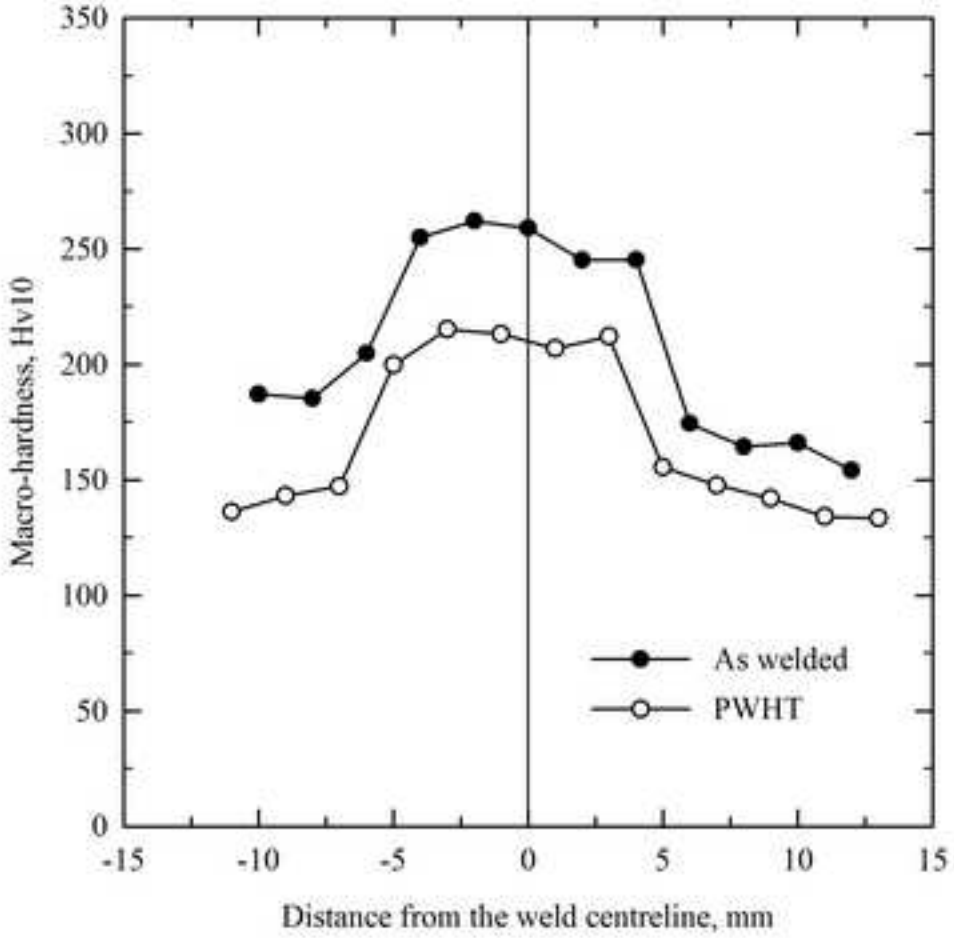

Figure 15
Click here to download high resolution image